





ARTICLE OPEN



The South America Low-Level Jet: form, variability and large-scale forcings

Charles Jones¹ , Ye Mu¹ , Leila M. V. Carvalho¹  and Qinghua Ding¹ 

Northerly low-level jets (LLJ) along the eastern Andes are important conduits of moisture transport and play central roles in modulating precipitation in South America. This study further investigates the variability of the LLJ during extended austral summers. A new method characterizes the spatial extent of the LLJ and finds four distinct types: Central, Northern, Andes and Peru. We show the existence of specific evolutions such that the LLJ may initiate in the central region, expands along the Andes and terminates in the northern region. Conversely, the LLJ may propagate from north-to-south. The spatiotemporal evolution of the LLJ is remotely forced by Rossby wave trains propagating from the Pacific Ocean towards South America, and the different phases of the wave trains favor the occurrences of Central, Northern or Andes types. Occurrences of Central and Northern types are more frequent in El Niño and La Niña years, respectively. The persistence of precipitation is shown to be directly related to the persistence of the LLJ. Lastly, the Madden-Julian Oscillation plays an important role in generating wave trains modulating the frequency of LLJ, especially the Central type.

npj Climate and Atmospheric Science (2023)6:175; <https://doi.org/10.1038/s41612-023-00501-4>

INTRODUCTION

Low-level jets are important conduits of moisture transport in tropical regions and play central roles in modulating precipitation, especially in monsoon systems^{1–6}. In this study, we focus on northerly low-level jets on the eastern slopes of the Andes (hereafter, LLJ). The South America Low-Level Jet (SALLJ) on the eastern slopes of the central Andes near Bolivia is a key component of the South American Monsoon System (SAMS)^{4,5,7–9}. Large and intense mesoscale convective systems (MCS) are typically formed in the exit region of the SALLJ^{10–13}. Oftentimes, MCS are associated with extreme weather^{10,14} causing significant socioeconomic impacts over the La Plata drainage basin and south-southeast Brazil.

The term SALLJ usually refers to the year-round northerly LLJ occurring to the east of the central Andes in Bolivia, northern Argentina and Paraguay. Conversely, the northerly LLJ on the eastern slopes of the Andes in Colombia and Venezuela is known as Orinoco jet^{15–19}. The LLJ in the central and northern Andes (i.e., central and northern branches) have been traditionally investigated separately. However, Jones (2019) provided a new understanding of the northerly LLJ in the eastern Andes and showed that the seasonal frequency of the LLJ in both regions are equally high and occasionally physically connected. They may occur independently or simultaneously in both regions, playing various roles in the distribution of precipitation in the SAMS. This new view allows new scientific opportunities to improve our understanding of the variability of these jets and their importance for the South America hydroclimate. For simplicity, we refer to the Orinoco jet as the Northern jet, which occurs along the eastern Andes from Venezuela, Colombia and northeast Peru. Likewise, we refer to the SALLJ as the Central jet. Additionally, we call central and northern branches as the corresponding regions of the Andes.

In this study, we further investigate the variability of the LLJ during extended austral summers (November–March), since this integrated view may aid us better understand the forming mechanisms of the jet and complex connections between jets

along the eastern slopes of the Andes. This overarching research goal is achieved by first employing a new method to characterize the spatial extent of LLJ and classify them into different types. Additionally, we show the existence of specific evolutions. In the Central-to-Northern evolution, the LLJ occurs initially only in the central region. A few days later, it may occur in the northern branch so that it is simultaneously present in both regions. Subsequently, it ends in the Central region and persists for a few more days in the northern branch, where it finally ends. Conversely, the Northern-to-Central evolution is similar but occurring in the reverse direction.

Previous studies have shown that the Central LLJ exhibits large variability on intraseasonal, interannual and multidecadal time scales^{5,7,8,18,20–23}. Therefore, this study also investigates large-scale forcings of the LLJ associated with the Madden-Julian Oscillation (MJO)²⁴ and El Niño/Southern Oscillation (ENSO)²⁵. We show that extratropical Rossby wave trains propagating across South America strongly modulate the occurrence of the Northern and Central LLJ types. Lastly, we discuss that the different LLJ types have markedly distinct influences on precipitation patterns over South America. All these analyses collectively present a broader view of the northerly LLJ in the climatology of the SAMS and over a broad range of time scales, which will facilitate future endeavors in improving simulations and predictions of the phenomenon.

RESULTS

Form and variability of northerly low-level jets

The climatology of nighttime winds (850-hPa) (Fig. 1) shows that easterly winds in the equatorial Atlantic veer to northerly directions as they reach South America, partially due to the blocking effect of the Andes Mountains. However, other physical processes and dynamical mechanisms may explain the jet's variability on multiple scales, and those will depend on the jet's strength and spatiotemporal characteristics^{21,26}. To identify and categorize nighttime occurrences of northerly LLJ, we developed

¹Department of Geography, University of California, Santa Barbara, CA, USA. ✉email: cjones@eri.ucsb.edu

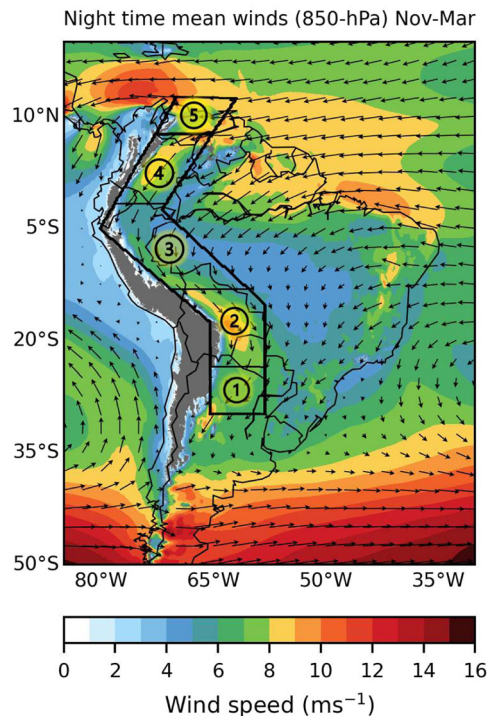


Fig. 1 Nighttime climatology of winds at 850-hPa during 1 November–31 March, 1979–2021. Nighttime corresponds to 23 UTC–09 UTC (19:00–05:00 Bolivia local time). Regions 1–5 indicate the mask used to identify LLJ days.

an algorithm that incorporates the jet structure, magnitude and spatial extensions along the eastern Andes (Supplementary Fig. 1). The method considers contiguous regions of wind speeds (CRWS) at 850-hPa greater than 10 m s^{-1} , the magnitudes of wind speeds (850-hPa) and vertical wind shear (700–850 hPa). Using this algorithm, four main types of SALLJ are defined. In the Central type, the LLJ extends only over southeast Peru, Bolivia, northern Argentina and Paraguay (Fig. 1, regions 1,2,3). Note that in any given Central type day, the LLJ may not necessarily extend over all three regions simultaneously. Instead, the jet may extend over different combinations of regions; the algorithm identifies these situations (see Methods). The second type is defined as the Northern LLJ, which extends over northern Peru, Colombia and Venezuela (Fig. 1, regions 3,4,5). The third type, denoted as Andes, is defined when low-level jets occur simultaneously in the northern and central branches. Note also that in the Andes type, the low-level jet may or may not extend along the entire eastern Andes. In the most frequent Andes type cases, the LLJ occurs simultaneously in the northern and central Andes but is absent over eastern Peru. In a subtype of the Andes type, denoted Andes-X, the LLJ is substantially intense and cover the entire extension of the eastern Andes. The fourth type, denoted as Peru, occurs much less frequently, is short-lived and covers only eastern Peru (Fig. 1, region 3). The Peru type is classified as a separate type to avoid the arbitrary decision of including it as a Central or Northern type, which would bias statistical analyses discussed next.

Figure 2 shows composites of winds at 850-hPa during Central, Northern, Andes types, and the Andes-X subtype; Supplementary Fig. 2 shows the Peru type.

To illustrate differences among the LLJ types, Fig. 3 shows the spatiotemporal evolutions of two LLJ events. In the first example (Fig. 3a), a Central type has a well-defined CRWS over southeastern Peru and Bolivia. Grid points satisfying low-level jet definitions (see Methods) are only present on the eastern part of the CRWS. In the next day (Fig. 3b), the LLJ intensified and expanded

considerably, forming an Andes type with spatially disconnected low-level jets in the northern and central Andes. The LLJ subsequently ceased in the central region and remained present in eastern Peru, Colombia and Venezuela (Fig. 3c). In a contrasting evolution (Fig. 3d–f), the LLJ started as a Northern type and evolved into Andes-X several days later. Subsequently, the LLJ evolved to a Central type. The LLJ was particularly active during December 2016.

These examples suggest that the LLJ may exhibit distinct evolutions along the eastern Andes, i.e., the LLJ may transition differently from one type to another and, interestingly, may evolve from south to north or vice versa. To investigate this problem, conditional probabilities are calculated to express the likelihood of initiation, transition between types and termination of the LLJ (Table 1). The 1st row shows the likelihood of LLJ initiation in a given type. We note that the LLJ is more likely to initiate as Central or Northern types (1st row, 0.295*, 0.117#, respectively) rather than Peru or Andes types. If initiated as Central type, it is more likely to persist in the same type (0.554), transition to Andes type (2nd row, 0.200*) or terminate (0.181). If an Andes type, it may stay in the same type (5th row, 0.611), transition back to Central (0.148) or change to Northern type (0.181*). Likewise, if initiated as Northern type (1st row, 0.117#), it is more likely to transition to Andes type (3rd row, 0.277#) and subsequently to Central type (5th row, 0.148#). Table 1 also shows the likelihood of the LLJ to persist in the same type (main diagonal) or to terminate (1st column, rows 2–5). The results support the hypothesis that the LLJ may follow two more likely pathways: *No-LLJ* \Rightarrow *Central* \Rightarrow *Andes* \Rightarrow *Northern* or *No-LLJ* \Rightarrow *Northern* \Rightarrow *Andes* \Rightarrow *Central*, indicating south-to-north or north-to-south evolutions.

Large-scale controls of northerly low-level jets

While boundary layer processes are important local mechanisms generating nocturnal low-level jets²⁷, large-scale processes may control the variability of the LLJ. Figure 4 shows composites of meridional winds (850-hPa, V850), zonal winds (200-hPa, U200) and geopotential height (200-hPa, Z200) anomalies during Central, Northern and Andes types. In all LLJ types, V850 anomalies show wave train activity originating in the South Pacific. In the Central type (Fig. 4a), as expected, negative V850 anomalies extend from the central Andes towards the South Atlantic, whereas positive V850 anomalies are observed over the northern Andes. An opposite pattern is observed during Northern type (Fig. 4c), where cross equatorial negative V850 anomalies favor the formation of the LLJ in the northern Andes and positive V850 anomalies inhibit the formation of Central type. During Andes type (Fig. 4e), negative V850 anomalies originate in the North Atlantic, cross the equator and flow along the eastern Andes towards the South Atlantic, thus favoring the simultaneous LLJ formation in the northern and central branches of the Andes. In the upper levels, all LLJ types also show wave train activity originating in the South Pacific. In the Central type (Fig. 4b), negative and positive Z200 anomalies over southern South America straddle positive U200 anomalies, indicating an enhancement of the subtropical jet. We note also that the pattern of Z200 anomalies suggests equatorial forcing over Indonesia. In the Northern type (Fig. 4d), similar wave train activity is present, but the important feature to note is that the phase of Z200 anomalies arriving in southern South America is opposite of the Central type. A somewhat different wave train activity pattern is observed during Andes type (Fig. 4f), where Z200 anomalies propagate more zonally than in the Central and Northern types, and positive Z200 anomalies are located over the South Atlantic rather than over the continent.

Figure 5 shows the annual distributions of Central, Northern and Andes types as functions of El Niño, neutral and La Niña years. Figure 5a suggests that El Niño favors the occurrence of the

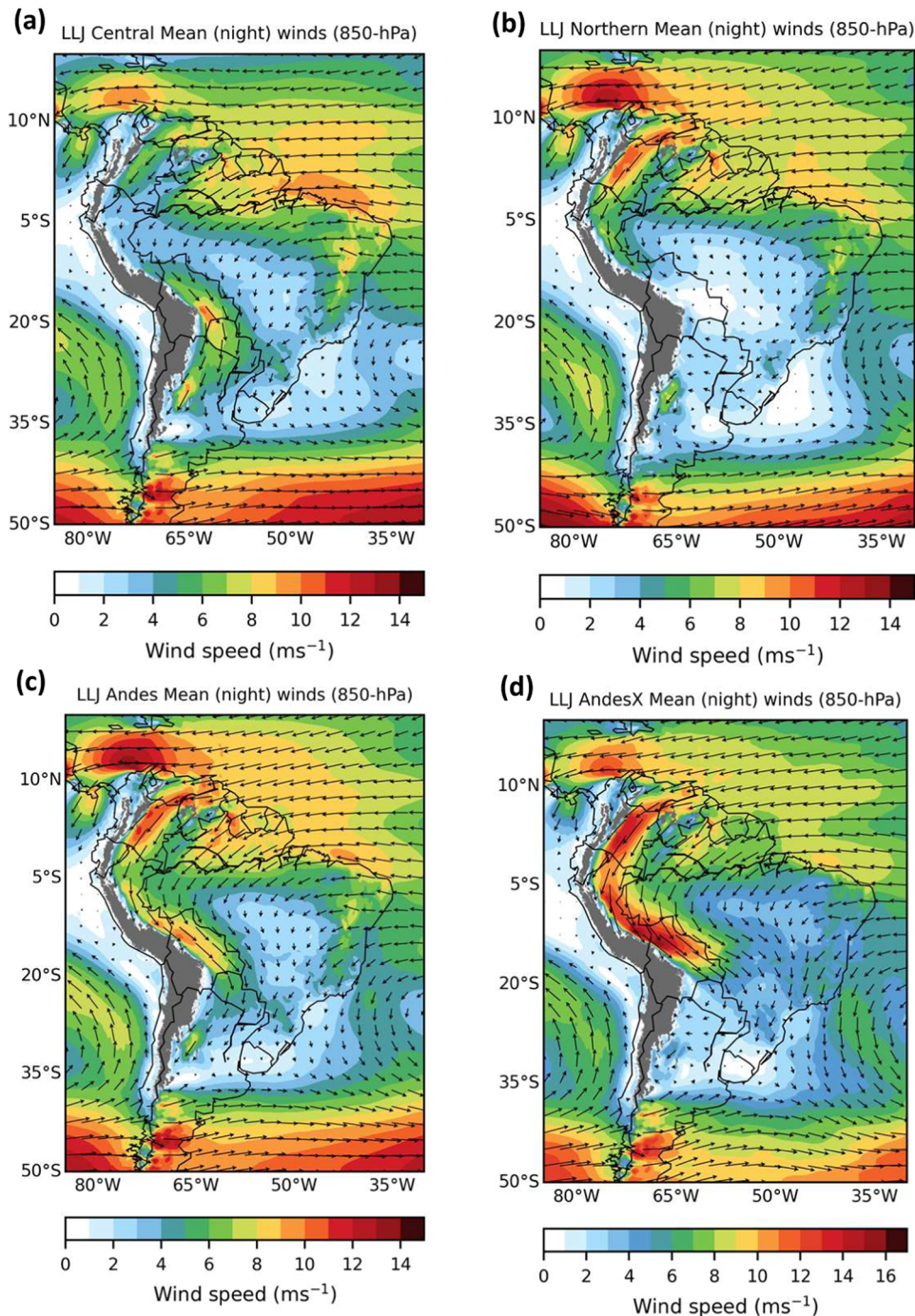


Fig. 2 Northerly low-level jet types. Composites of winds at 850-hPa during (a) Central, (b) Northern, (c) Andes types and (d) Andes-X LLJ sub-type.

Central type; this is especially the case during strong El Niño years (i.e., 82–83, 86–87, 97–98, 09–10, 15–15). In contrast, La Niña years appears to favor the occurrence of the Northern and Andes types (Fig. 5b, c). Supplementary Table 1 shows the percentages of LLJ types with ENSO phases. El Niño and La Niña years increase the frequencies of Central and Northern types, respectively. However, the difference between El Niño and La Niña is statistically significant (10% level) only for the Central type. The results above motivate the investigation of these two questions: 1) Is the wave train activity (Fig. 4) higher during La Niña or El Niño years? 2) Does ENSO modulate the persistence of LLJ types?

To investigate the first question, we calculate an empirical orthogonal function (EOF) analysis of Z200 anomalies during all days of Central type. To emphasize the southern hemisphere wave train, the domain is bounded between 10°S–80°S. The first two EOF modes are shown in Supplementary Fig. 3. They represent 10% and 8% of the total variance of Z200 anomalies. If the EOF analysis is done using the Northern type days, the EOFs are essentially the same but with opposite signs. We project all days of Z200 anomalies onto the first two EOF modes resulting in two time series PC1 and PC2, and calculate $PC = \sqrt{PC1^2 + PC2^2}$. Next, we calculate the percentage of days during La Niña, neutral and El

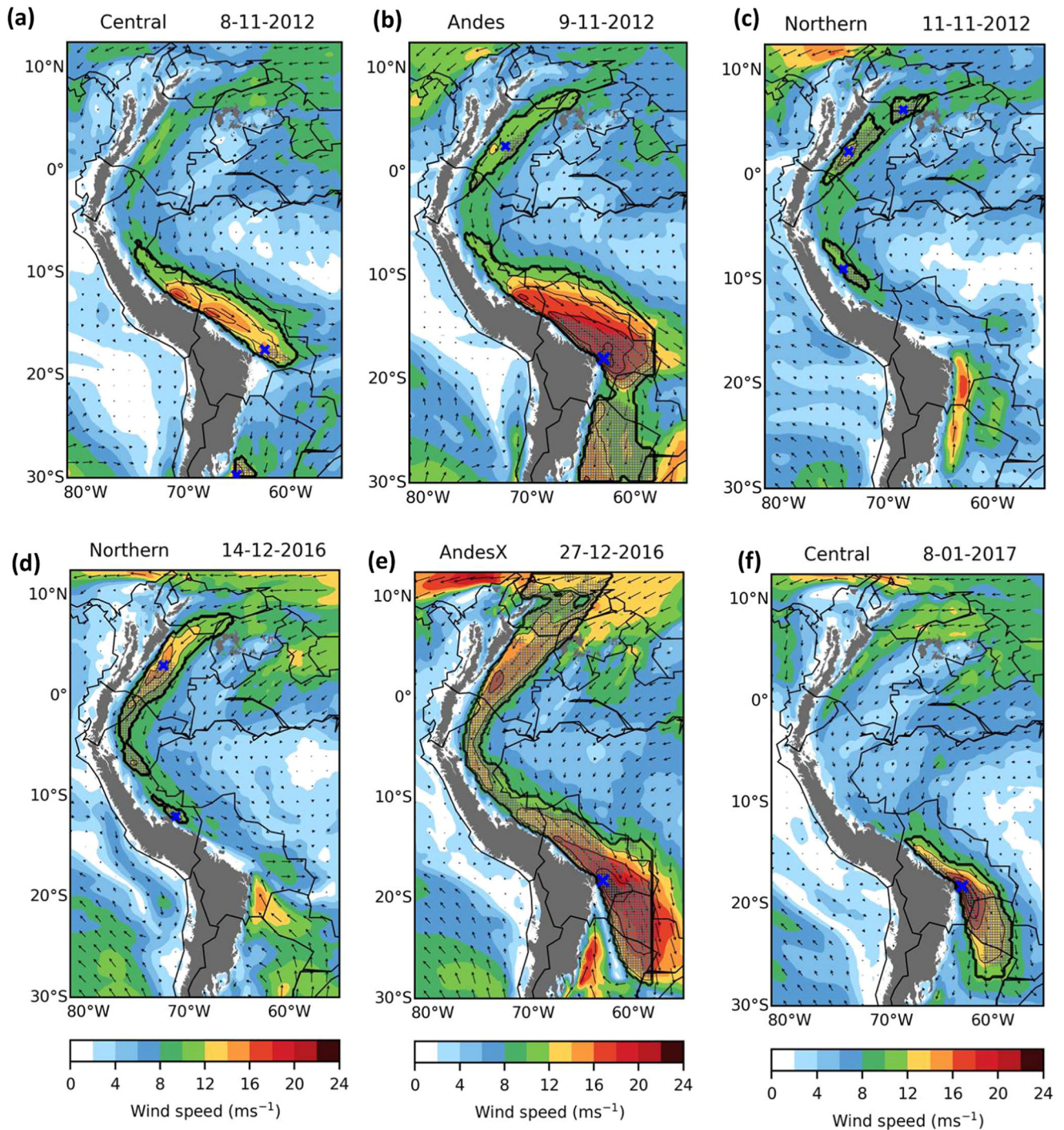


Fig. 3 Examples of LLJ transitions. Top row shows transitions from (a) Central to (b) Andes to (c) Northern types. Bottom row shows transitions from (d) Northern to (e) Andes-X to (f) Central type. Thin black lines show contiguous regions with wind speeds equal or greater than 10 m s^{-1} . Hatching shows grid points satisfying both wind speed and vertical wind shear criteria within contiguous regions with wind speeds equal or greater than 10 m s^{-1} . Blue “X” shows the core of the LLJ: location of maximum wind speed (850-hPa) within the LLJ.

Niño years in which PC is greater than the 75th percentile of the frequency distribution. The results indicate that wave train activity is higher during La Niña (40.4%) than in El Niño (30%) years.

We calculate persistence as the number of consecutive days in each LLJ type (1 day minimum duration). We then separate the persistences for each LLJ type according to El Niño, neutral and La Niña years and compute interquartile ranges, means, 90th, 95th percentiles and maximum durations (Fig. 6). ENSO has a distinct influence on the distribution of LLJ persistences. La Niña years

favor long persistences of the Northern type, whereas El Niño years favor long persistences of the Central, which is particularly noted in the 90th and 95th percentiles and maxima persistences.

Additional understanding about interannual changes in the large-scale circulation and LLJ types is demonstrated by compositing daily meridional winds (850-hPa, V_{850}), Z200 and OLR anomalies on Central, Northern and Andes types. Composites are stratified by La Niña, neutral and El Niño years. During Central type (Supplementary Fig. 4) and all ENSO phases (Fig. S4a, c, e), broad

regions of negative V850 anomalies extend from the central Andes towards the South Atlantic, thus favoring the formation of the Central type. In contrast, positive V850 anomalies suppress the LLJ formation in the northern Andes. The V850 wave train patterns

Table 1. Transition probabilities between different LLJ types: Central, Northern, Peru and Andes.

		X_{t+1}				
		No-LLJ	Central	Northern	Peru	Andes
X_t	No-LLJ	0.494	0.295*	0.117#	0.015	0.078
	Central	0.181	0.554	0.062	0.004	0.200*
	Northern	0.172	0.093	0.454	0.004	0.277#
	Peru	0.306	0.286	0.163	0.061	0.184
	Andes	0.053	0.148#	0.181*	0.007	0.611

The first column on the left and first row on top indicate the states at X_t and X_{t+1} , respectively. Numbers in bold in the main diagonal indicate conditional probabilities to persist in the same state. Bold numbers with * symbol indicate the likelihood for the transition: $No-LLJ \Rightarrow Central \Rightarrow Andes \Rightarrow Northern$. Bold numbers with # symbol indicate the likelihood for the transition: $No-LLJ \Rightarrow Northern \Rightarrow Andes \Rightarrow Central$.

indicate remote forcing from the Pacific Ocean. During La Niña years (Fig. S4b), negative OLR anomalies are located over Indonesia and Z200 anomalies extend from the South Pacific towards South America. During neutral years (Fig. S4d), negative OLR anomalies are in the western Pacific and an enhanced Pacific South American (PSA) pattern forces Z200 anomalies propagating over South America. Negative OLR anomalies over the Central Pacific during El Niño are associated with Z200 anomalies emanating to South America (Supplementary Fig. 4f). Supplementary Figs. 5 and 6 show composites of Northern and Andes types as functions of ENSO phases. While El Niño and La Niña years change the climatological location of tropical convective activity and basic state, these results show that for the same type of LLJ, the spatial patterns and magnitudes of the wave trains in Z200 anomalies are not modified by ENSO. In contrast, ENSO influences the activity of the wave train and persistence of LLJ, such that the Central type is skewed by El Niño years, whereas the Northern type is skewed by La Niña years.

On subseasonal time scales, the MJO is a fundamental mode influencing global weather-climate variability (see also Supplementary Fig. 7). To gain further understanding on MJO and LLJ relationships, Fig. 7 shows the distributions of Central, Northern and Andes types versus MJO phases. They are constructed by counting the number of LLJ days in that type and phase, and

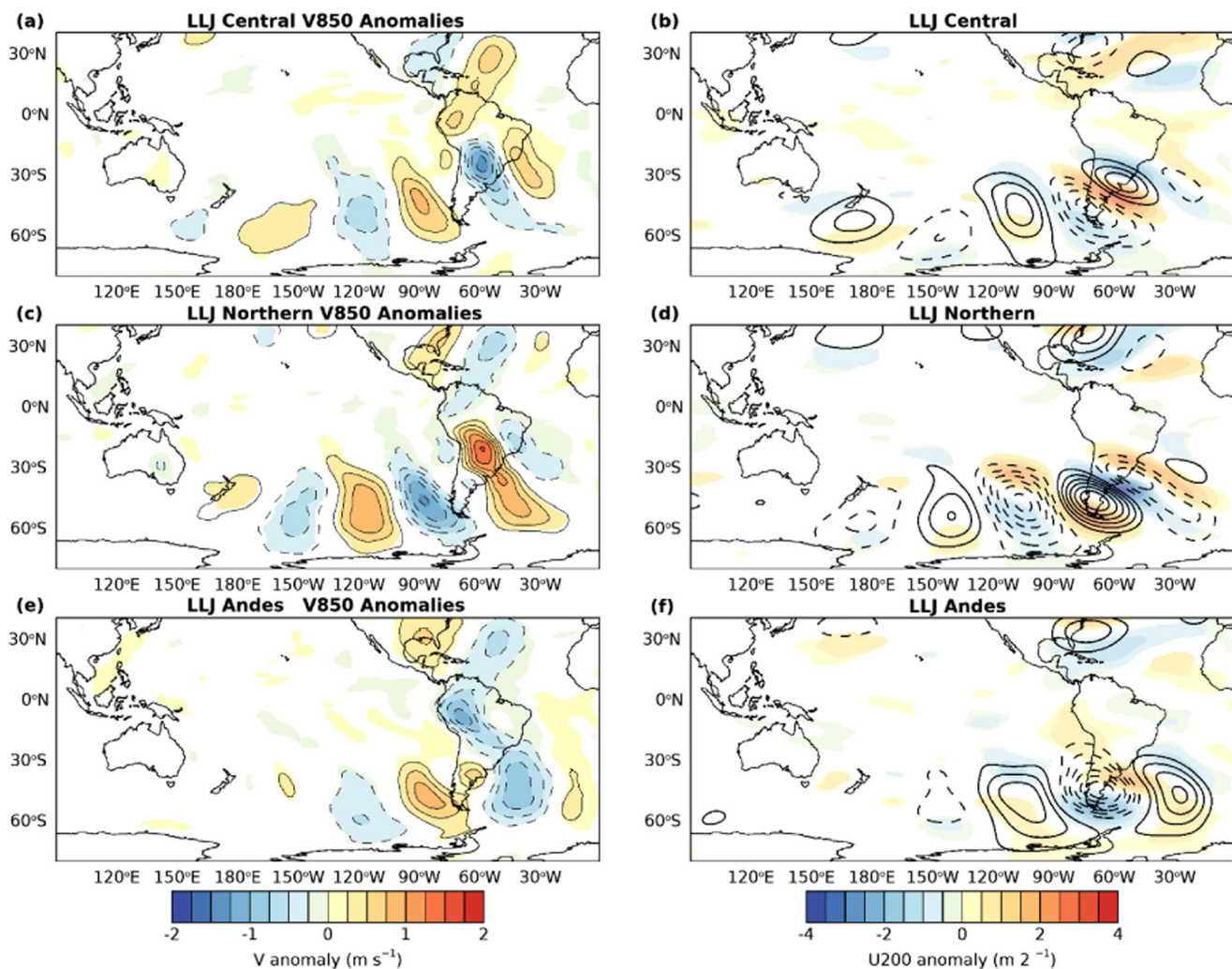


Fig. 4 Composites of LLJ Central (top row), Northern (middle row) and Andes (bottom row) types. Left column: meridional wind (850-hPa) anomalies; Right column: zonal wind (200-hPa) (colors) and geopotential height (200-hPa, Z200) (contours) anomalies. Positive (negative) Z200 anomalies are shown in solid (dashed) contours (5 m interval); zero contour omitted. Anomalies are statistically significant at 5% level.

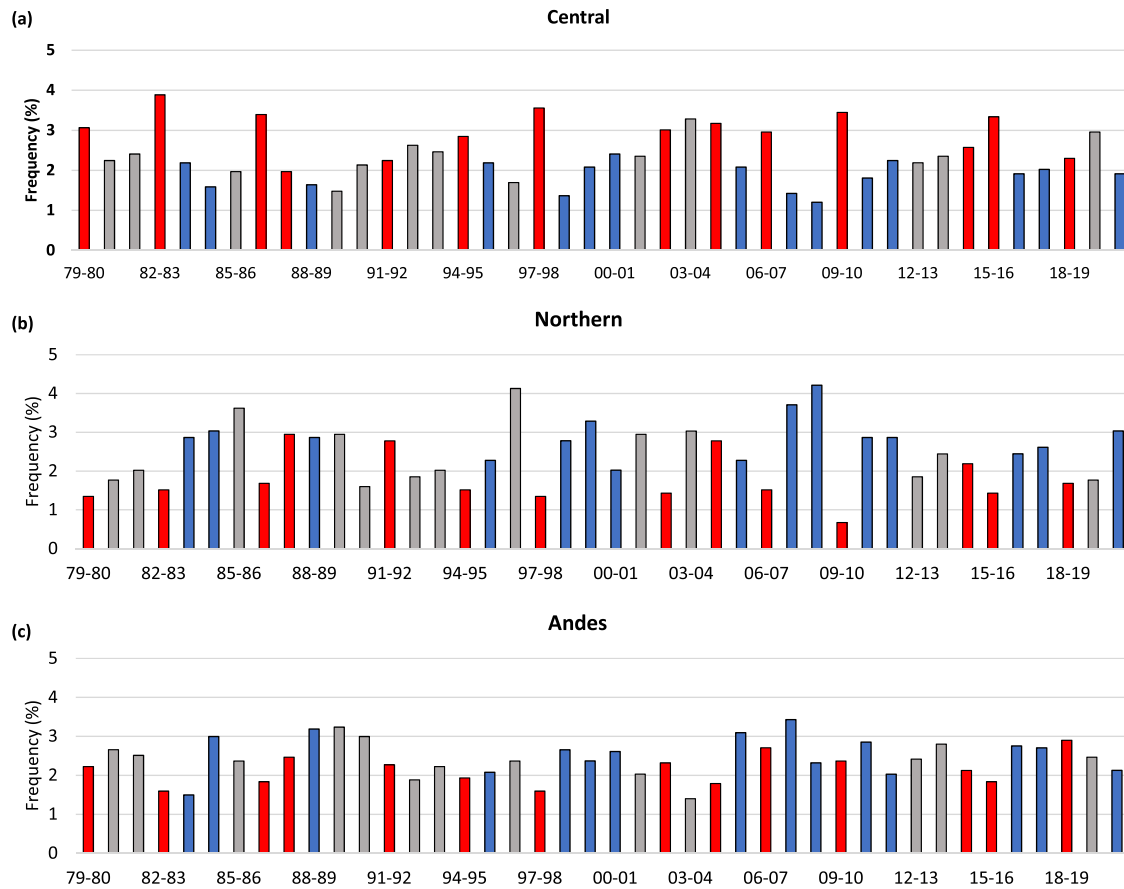


Fig. 5 Interannual variability of LLJ types. Annual frequency distributions of LLJ types: **a** Central, **b** Northern and **c** Andes types. El Niño, neutral and La Niña years are indicated by red, gray and blue bars, respectively. Period: 1 November–31 March.

dividing by the total number of LLJ type days. The mean frequency is removed for easier interpretation. The influence of the MJO on the Central type occurs in phases 5–6 (Fig. 7a), when the MJO convective signal is over Indonesia (Supplementary Fig. 7). In the Northern type (Fig. 7b), the highest frequencies are in phases 1 and 4–6, when enhanced convection is in the western Pacific or propagating from the Indian Ocean to Indonesia. Supplementary Fig. 8 shows composites of OLR and Z200 anomalies during Central type and MJO phases 4, 5 and 6, and show the evolution of the wave train reaching South America. Unlike in the Central type, where there is a systematic shift from negative-to-positive-to-negative anomalies in the frequencies, the Northern type is influenced by the MJO and synoptic variability unrelated to the MJO. In contrast, a systematic shift in the Andes type frequencies shows a control by the MJO when enhanced convection intensifies and propagates eastward over the Indian Ocean (Fig. 7c, Supplementary Fig. 7).

The distributions of LLJ types as functions of MJO phases during warm and cold ENSO are shown in Supplementary Fig. 9. The MJO influences the Central type preferentially in phase 6 (convective anomalies over Indonesia) during El Niño, whereas it changes to phase 5 during La Niña years. This change is consistent with the westward retraction of mean convection during La Niña years. For Northern type, the frequency distributions are more evenly distributed with MJO phases during El Niño and La Niña years. It is difficult to judge any preferential MJO phase for Andes types during El Niño years, highlighting complex non-linear interactions between these two modes of climatic variability. In contrast, during La Niña years, the Andes type are more frequent in phase 3, when the enhanced MJO convection is over the Indian Ocean.

Northerly low-level jets and precipitation variability in South America

It is clear from the results aforementioned that northerly low-level jets along the eastern Andes may occur independently or simultaneously in the northern and central branches of the Andes. Figure 8 shows precipitation anomalies during Central, Northern and Andes types from two datasets. Consistent with previous studies^{10,20}, when the LLJ is present only in the central Andes (Fig. 8a, d), precipitation enhancement is observed over the La Plata Basin. Moreover, positive precipitation anomalies are found in the northern Andes; negative precipitation anomalies over the Amazon and southeast Brazil indicate suppression of the South Atlantic Convergence Zone (SACZ)²⁸. In contrast, during Northern types (Fig. 8b, e), precipitation is enhanced over the Amazon, whereas precipitation decreases over the La Plata Basin and northern Andes. Positive anomalies are particularly large over most of eastern Peru and northern Bolivia, which is related to the intense moisture transport by the LLJ and the blocking effect of the Andes. Note also that IMERG suggests an enhancement of oceanic SACZ²⁸. Distinct precipitation anomaly patterns are found during Andes type (Fig. 8c, f). While positive precipitation anomalies are found over the La Plata Basin, they are not as strong during Central types. Positive precipitation anomalies are small or not statistically significant over a large region over the Amazon Basin. It is worth noting that negative precipitation anomalies are enhanced over northern South America over a larger area than during Northern type.

The previous results show that cold and warm ENSO phases control the activity of wave trains and persistence of Northern and Central LLJ types. To investigate potential ENSO influences on the persistence of precipitation during LLJ types, we select the two

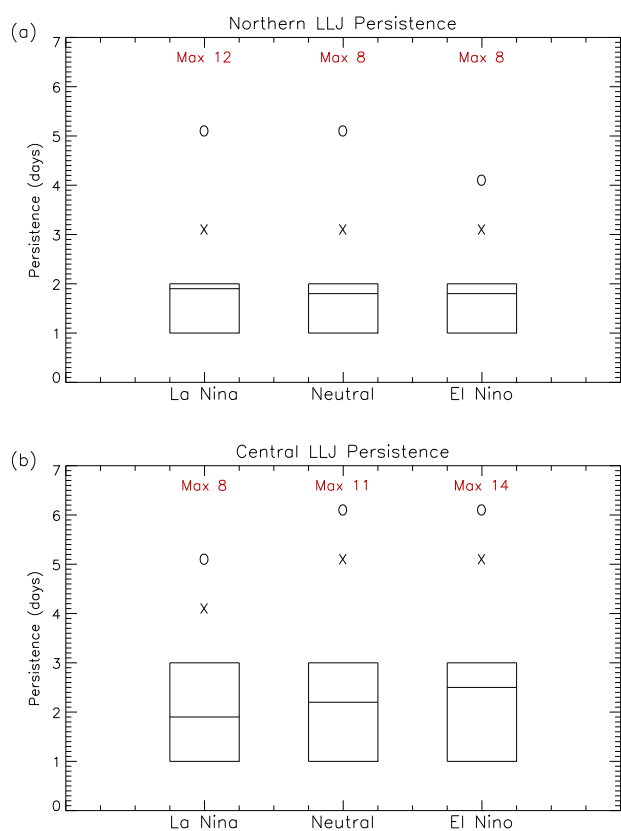


Fig. 6 Persistence of LLJ types and ENSO phases. Distributions of persistence of (a) Northern and (b) Central types. Distributions are calculated separately during La Niña, Neutral and El Niño years as indicated in the horizontal axis. Box indicates the interquartile range; the horizontal line within the box shows the mean persistence. X and O symbols indicate the 90th and 95th percentiles; maximum persistence is shown in red.

domains indicated in Fig. 8d, e. In each region, daily mean precipitation is computed by spatially averaging gridpoints with precipitation above 1 mm. CHIRPS is used because there is a longer record than IMERG. Persistence is calculated as the number of consecutive days with precipitation greater than 1 mm (1 day minimum). Calculations are done separately for Northern and Central types, and El Niño, neutral and La Niña years. During Northern types (Fig. 9a), La Niña years favor precipitation events with longer durations than in El Niño years. In contrast, during Central types (Fig. 9b), El Niño years favor persistences with longer duration than in La Niña years. This ENSO influence is particularly noticeable in the tails (90th and 95th percentiles and maxima) of the frequency distributions of persistence.

DISCUSSION

Northerly low-level jets along the eastern Andes have long been recognized as important in transporting moisture, particularly moisture carried by the Atlantic easterly winds entering the continent and moisture from Amazon evaporation, and, therefore, controlling the water balance^{6,19,29}. Previous studies investigated the formation and variability of LLJ separately in the northern (Orinoco) and central branches of the Andes. Jones (2019), however, pointed out that the seasonal frequency of the LLJ in both regions are equally high, and jet occurrences may occur independently or simultaneously in both regions.

This study reemphasizes an integrated view by identifying the spatial extent of LLJ as they occur in the northern-to-central eastern Andes. Although the extent of LLJ varies significantly from

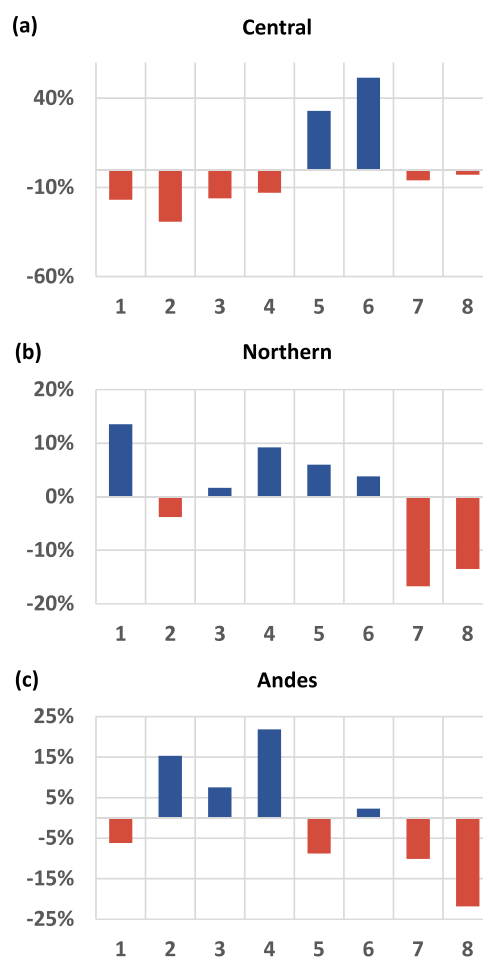


Fig. 7 Distributions of LLJ types and MJO phases. Anomalous frequencies of LLJ occurrences as a function of MJO phases during (a) Central, (b) Northern and (c) Andes types. Anomalies were computed as [number of occurrences in a given phase – mean occurrences in all phases] / [mean occurrences in all phases].

event to event, four types are identified. Consistent with previous studies, the Central type is active over southeastern Peru, Bolivia and Paraguay. The Northern type, in contrast, is active only in northern Peru, Colombia and Venezuela and is traditionally referred to as Orinoco low-level jet. The Andes type is characterized by simultaneous occurrences of low-level jets in the northern and central Andes. The Peru type occurs only in central eastern Peru. They are typically short-lived and have small spatial extent. This study classifies this type as a separate entity to avoid the arbitrary decision of classifying it as Central or Northern, which could introduce noise in the statistical analyses presented here. We hypothesize that the Peru type is driven by local boundary layer processes and not sensitive to large-scale forcing mechanisms. This aspect of the Peru type could be an interesting topic for future investigations. Interestingly, a subset of the Andes type, defined as Andes-X, is characterized by LLJ extending over the entire eastern Andes. This subtype exhibits substantially higher wind speeds (850-hPa) than the other types.

This study additionally shows that there are distinct pathways for the LLJ spatiotemporal evolution. The LLJ may start in the central (or northern) Andes and remain confined to that geographic region. However, a south to north evolution has also been identified, in which the LLJ starts as Central type, transitions to Andes and subsequently to Northern type. Conversely, in the north to south transition, the LLJ initiates in the northern Andes, transitions to Andes and Central types.

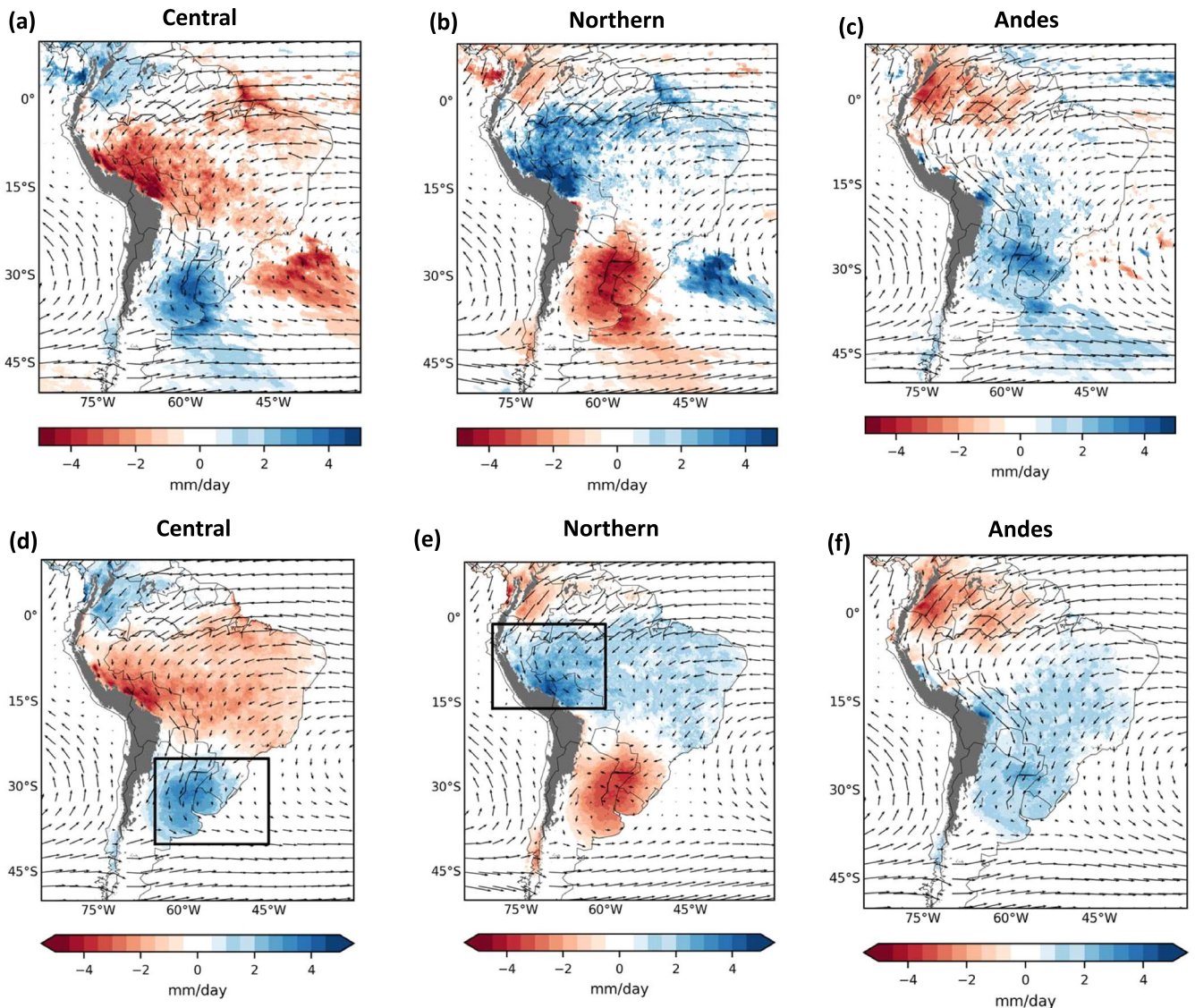


Fig. 8 Composites of precipitation anomalies (mm day^{-1}) and winds (850-hPa) (m s^{-1}) during Central, Northern and Andes LLJ types. Panels (a–c) show composites based on IMERG and (d–f) on CHIRPS data. Boxes in (d) and (e) are used to calculate persistence of precipitation during LLJ types shown in Fig. 9.

The spatiotemporal evolution of the LLJ is remotely forced by large-scale dynamics on intraseasonal-to-interannual time scales. The Central type is favored when Rossby wave trains induce negative and positive Z200 anomalies and an intensification of the subtropical jet (U200) over southern South America (Fig. 4b). This is consistent with Liebmann et al. (2004) who investigated subseasonal variations in precipitation over the La Plata Basin and SACZ (see their Fig. 9). In contrast, the Northern type is favored when Rossby wave trains induce positive and negative Z200 anomalies and weakening of the subtropical jet (U200) over southern South America (Fig. 4d). A somewhat different wave train activity pattern is observed during Andes type (Fig. 4f), where Z200 anomalies propagate more zonally than in the Central and Northern types, and positive Z200 anomalies are located over the South Atlantic rather than over the continent.

This study also identifies important relationships between LLJ and ENSO. In the 43 years of data analyzed, the distribution of Central type is skewed by ENSO such that, in agreement with previous studies^{5,23,30}, El Niño years favor an increase in the frequency of Central type. Conversely, the distribution of Northern type is skewed by La Niña years. Although the result is not

statistically significant, La Niña years increase the frequency of Northern type, which is consistent with Builes-Jaramillo et al. (2022). The skewness of the frequency distribution of Central type by El Niño comes from long LLJ durations. Likewise, the skewness of the Northern type frequency comes from very long LLJ durations during La Niña years. We additionally found that El Niño and La Niña years do not modify the spatial structure and magnitudes of the corresponding Rossby wave train patterns for the different LLJ types. The wave train patterns are, however, significantly more active in La Niña than El Niño years.

On intraseasonal time scales, the MJO has also an important modulation on the LLJ types. The LLJ can occur in all phases of the MJO life cycle. However, the frequencies of Central and Northern types increase when MJO convective activity is located over the eastern Indian Ocean and Indonesia. The frequency of Andes type increases when MJO convective activity is propagating eastward over the Indian Ocean.

The Northern, Central and Andes LLJ types are associated with distinct precipitation patterns over South America. El Niño and La Niña years have distinct controls on the duration of the Northern and Central LLJ types and consequently on the persistence of

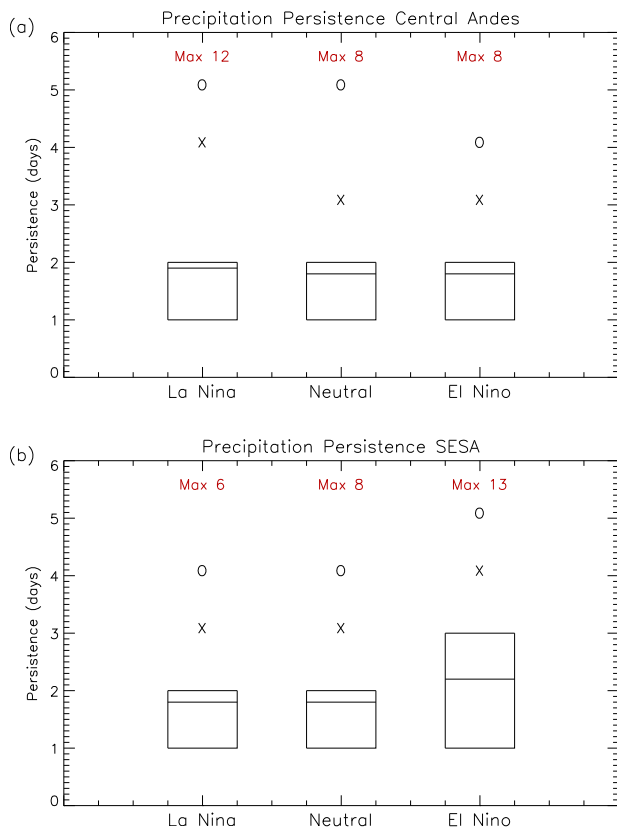


Fig. 9 Persistence of precipitation during LLJ types and ENSO phases. Distributions of persistence of precipitation during (a) Northern and (b) Central types. Distributions are calculated separately during La Niña, Neutral and El Niño years as indicated in the horizontal axis. Box indicates the interquartile range; the horizontal line within the box shows the mean persistence. X and O symbols indicate the 90th and 95th percentiles; maximum persistence is shown in red. SESA is Southeast South America.

precipitation events. This study suggests that monitoring large-scale intraseasonal-to-interannual tropical convective anomalies can provide important guidance to develop subseasonal-to-seasonal forecasts over South America. Our study is the first study of its kind clearly demonstrating these circulation-precipitation interaction processes, which may serve as an observational benchmark for future efforts in evaluating climate models' performance in simulating the same processes. Our analysis mainly focuses on prevailing tropical Pacific conditions related to ENSO and MJO in shaping the four different types of northerly low-level jets. Other climate drivers such as sea surface temperature modes over the tropical Atlantic and extratropical South Atlantic, the southern annular mode, and many other atmospheric circulation modes in the southern hemisphere may also apply remote forcings on jet variability, which needs more attention in future studies.

METHODS

Low-level jet identification

The identification of the LLJ, its form, variability and large-scale forcings are investigated with European Centre for Medium-Range Weather Forecasts ERA5 reanalysis³¹. Hourly averages of zonal and meridional wind components at 850-hPa and 700-hPa (U850, V850, U700, V700) and geopotential height at 200-hPa (Z200) are used during extended austral summers (1 November–31 March, 1979–2021). Montini et al. (2019) showed that vertical wind profiles

from modern reanalyses compare very well with radiosonde observations during the South American Low-level Jet Experiment (SALLJEX).

To identify LLJ occurrences and its spatial forms, we first compute nighttime averages of U850, V850, U700 and V700 during 23–09 UTC (19:00–05:00 Bolivia local time). LLJ are identified in every grid point within the (30.0S–12.5 N; 81.75W–55.0 W) domain. We define a low-level jet when the nighttime wind speed (850-hPa) and wind shear between 850-hPa and 700-hPa exceed the corresponding 75th percentiles of the monthly frequency distributions. The spatial extent of LLJ is determined by using a mask along the eastern Andes (Fig. 1); the mask has five subdivisions. We first identify contiguous regions of wind speeds at 850-hPa (CRWS) greater than 10 m s^{-1} overlapping any of the five subregions. Additional criteria include: a) the minimum size of 5 grid points in the CRWS and b) a minimum of 5 grid points with low-level jets within the CRWS. The minimum size of 5 grid points was deemed optimal and avoided situations when isolated grid points show low-level jets along the eastern Andes. The core of the LLJ is additionally defined by the grid point with the maximum wind speed (850-hPa). The definitions above seek to characterize the spatial form of regions with high wind speeds encapsulating regions with low-level jets. This characterization of the LLJ avoids the use of pre-determined fixed locations to identify low-level jets^{5–8,21,26}.

Low-level jet form

The spatial extent of the LLJ is classified into four types (Central, Northern, Andes and Peru) and based on the overlapping of the CRWS with the five subregions (Fig. 1). These five regions are defined based on the intensity of the nighttime climatological winds. If there is only one CRWS, it is classified based on the overlapping: Central (1, 2, 12, 23 or 123), Northern (4, 5, 45, 34 or 345), Andes (12345, 1234, 234 or 2345) and Peru (3). If there are more than one CRWS, they are classified based on the overlapping: a) Central (only Central or Central and Peru), b) Northern (only Northern or Northern and Peru), c) Andes (Central and Northern or any combinations of 12345, 1234, 234 or 2345). Supplementary Fig. 1 summarizes the main steps to identify LLJ. The frequencies of each type are: Central (36%), Northern (23%), Peru (1%) and Andes (40%) (2070 total cases). This shows that the LLJ can occur only in the Central, only in the Northern or simultaneously in the Northern and Central Andes. The Peru type is frequently associated with small regions of low-level jets forming off eastern Peru; they are also short-lived as shown next. A sub-category in the Andes type, denoted as Andes-X, occurs when one CRWS extends along the eastern Andes (12345, 1234, 234 or 2345). The frequency of Andes-X is 5.6% of the Andes types and they are associated with very high wind speeds. Figure 2 shows composites of winds at 850-hPa during Central, Northern, Andes and Andes-X types. Composites of Peru types are shown in Supplementary Fig. 1. Examples of LLJ types are shown in Fig. 3.

Low-level jet variability and large-scale forcings

The temporal evolution of the four LLJ types is modeled with a five-state first order Markov Chain approach^{32,33}. We consider a discrete time series with five possible states corresponding to LLJ types: 0=no-LLJ, 1=Central, 2=Northern, 3=Peru and 4=Andes. Conditional probabilities (P) are expressed as $\{X_{t+1} = S_j | X_t = S_i\}$, where $S_j = [0, 4]$, $S_i = [0, 4]$ are states ($P_{j,i} = [0, 4]$, $i = [0, 4]$). The conditional probabilities express the likelihood of initiation, transition from one type to another and termination of the low-level jet. Twenty-five conditional probabilities need to be estimated, one for each combination of $S_j S_i, j, i \in [0, 4]$ pair. Table 1 shows the transition probabilities.

To characterize large-scale forcings of the LLJ, daily V850 and Z200 are filtered. Only variations between 2.5–30 days and eastward propagating 1–15 zonal wavenumbers are retained. This filtering procedure is designed to focus on the influence of extratropical Rossby wavy trains on the LLJ^{20,34}.

Daily averages of outgoing longwave radiation (OLR)^{35,36} are used as a proxy for tropical convective activity (1 November–31 March, 1979–2021). OLR is filtered in two ways. To analyze MJO and LLJ relationships, a band-pass filter is applied in the frequency domain to retain variations between 20–90 days. To analyze ENSO and LLJ relationships, a low-frequency filter is applied to OLR to retain variations longer than 2 years. The classification from the Climate Prediction Center, National Centers for Environmental Prediction (<https://origin.cpc.ncep.noaa.gov/>), is used to select El Niño, neutral and La Niña years.

The OLR Madden-Julian Oscillation (OMI) index of Kiladis et al. (2014, 2020) is employed to study large-scale forcings of the LLJ associated with the MJO. The OMI index is used to characterize the life cycle of the MJO into eight phases following the methodology described in (Jones and Carvalho 2011) (Supplementary Fig. 7).

Daily precipitation data are from the Integrated Multi-satellite Retrievals for GPM (IMERG) V06B Final runs³⁷ and the Climate Hazards Group InfraRed Precipitation with Station data (CHIRPS)³⁸. IMERG daily was used at 0.1° resolution from 2000 to 2021, and CHIRPS was at 0.05° resolution from 1981 to 2021. Precipitation anomalies are computed as the difference between daily precipitation on SALLJ days minus no-SALLJ days.

DATA AVAILABILITY

The research presented here was derived from data sets that are all publicly available.

CODE AVAILABILITY

Interactive Data Language (IDL) computer code was used for data processing and analyses. Computer codes are available from the author upon reasonable request.

Received: 17 March 2023; Accepted: 16 October 2023;

Published online: 31 October 2023

REFERENCES

- Findlater, J. A major low-level air current near the Indian Ocean during the northern summer. *Q. J. R. Meteorol. Soc.* **95**, 362–380 (1969).
- Stensrud, D. J. Importance of Low-Level Jets to Climate: A Review. *J. Clim.* **9**, 1698–1711 (1996).
- Joseph, P. V. & Sijikumar, S. Intraseasonal variability of the low-level jet stream of the Asian summer monsoon. *J. Clim.* **17**, 1449–1458 (2004).
- Vera, C. et al. Toward a unified view of the American Monsoon Systems. *J. Clim.* **19**, 4977–5000 (2006).
- Montini, T. L., Jones, C. & Carvalho, L. M. V. The South American Low-Level Jet: a New Climatology, Variability, and Changes. *J. Geophys. Res.* <https://doi.org/10.1029/2018JD029634> (2019).
- Do Nascimento, M. G., Herdies, D. L., de Souza, D. O. & De Souza, D. O. The South American Water Balance: The Influence of Low-Level Jets. *J. Clim.* **29**, 1429–1449 (2016).
- Marengo, J., Soares, W. R., Saulo, C. & Nicolini, M. Climatology of the low-level jet east of the Andes as derived from the NCEP–NCAR reanalyses: Characteristics and temporal variability. *J. Clim.* **17**, 2261–2280 (2004).
- Vera, C. et al. The South American low-level jet experiment. *Bull. Am. Meteorol. Soc.* **87**, 63–77 (2006).
- Carvalho, L. M. V. & Cavalcanti, I. F. A. The South American Monsoons System (SAMS). In *The Monsoons and Climate Change: Observations and Modelling* (eds. Carvalho, L. M. V. & Jones, C.) 253 pp (Springer International Publishing, 2016).
- Salio, P. et al. Mesoscale convective systems over southeastern South America and their relationship with the South American low-level jet. *Mon. Weather Rev.* **135**, 1290–1309 (2007).
- Rasmussen, K. L. & Houze, R. A. Convective Initiation near the Andes in Sub-tropical South America. *Mon. Weather Rev.* **144**, 2351–2374 (2016).
- Romatschke, U. & Houze, R. A. Extreme Summer Convection in South America. *J. Clim.* **23**, 3761–3791 (2010).
- Romatschke, U. & Houze, R. A. Characteristics of Precipitating Convective Systems Accounting for the Summer Rainfall of Tropical and Subtropical South America. *J. Hydrometeorol.* **14**, 25–46 (2013).
- Gamelin, B. L., Carvalho, L. M. V. & Jones, C. Evaluating the influence of deep convection on tropopause thermodynamics and lower stratospheric water vapor: A RELAMPAGO case study using the WRF model. *Atmos. Res.* **267**, 105986 (2022).
- Espinoza, J. C. et al. Hydroclimate of the Andes Part I: Main Climatic Features. *Front Earth Sci.* **8**, 1–20 (2020).
- Torrealba, E. R. & Amador, J. A. La corriente en chorro de bajo nivel sobre los Llanos Venezolanos de Sur América. *Rev. de Climatol.* **10**, 1–20 (2010).
- Jiménez-Sánchez, G., Markowski, P. M., Young, G. S. & Stensrud, D. J. The Orinoco Low-Level Jet: An Investigation of Its Mechanisms of Formation Using the WRF Model. *J. Geophys. Res. Atmos.* **125**, e2020JD032810 (2020).
- Builes-Jaramillo, A., Yepes, J. & Salas, H. D. The Orinoco low-level jet during El Niño–Southern Oscillation. *Int. J. Climatol.* <https://doi.org/10.1002/JOC.7681> (2022).
- Martinez, J. A. et al. The Orinoco Low-Level Jet and the Cross-Equatorial Moisture Transport Over Tropical South America: Lessons From Seasonal WRF Simulations. *J. Geophys. Res.* **127**, 1–22 (2022).
- Liebmann, B., Kiladis, G. N., Vera, C. S., Saulo, A. C. & Carvalho, L. M. V. Subseasonal variations of rainfall in South America in the vicinity of the low-level jet east of the Andes and comparison to those in the South Atlantic convergence zone. *J. Clim.* **17**, 3829–3842 (2004).
- Jones, C. & Carvalho, L. M. V. The influence of the Atlantic multidecadal oscillation on the eastern Andes low-level jet and precipitation in South America. *NPJ Clim. Atmos. Sci.* **1**, 40 (2018).
- Petersen, W. A., Fu, R., Chen, M. & Blakeslee, R. Intraseasonal Forcing of Convection and Lightning Activity in the Southern Amazon as a Function of Cross-Equatorial Flow. *J. Clim.* **19**, 3180–3196 (2006).
- Bruick, Z. S., Rasmussen, K. L., Rowe, A. K. & McMurdie, L. A. Characteristics of Intense Convection in Subtropical South America as Influenced by El Niño–Southern Oscillation. *Mon. Weather Rev.* **147**, 1947–1966 (2019).
- Madden, R. A. & Julian, P. R. Observations of the 40–50-Day Tropical Oscillation-A Review. *Mon. Weather Rev.* **122**, 814–837 (1994).
- Ropelewski, C. F. & Arkin, P. A. *Climate Analysis. Climate Analysis* (Cambridge University Press, 2019). <https://doi.org/10.1017/9781139034746>.
- Jones, C. Recent changes in the South America low-level jet. *Nature Climate and Atmospheric Science* <https://doi.org/10.1038/s41612-019-0077-5l> (2019). 10.1038/s41612-019-0077-5.
- Stull, R. B. *An Introduction to Boundary Layer Meteorology*. (Kluwer Academic Publishers, 1999).
- Carvalho, L. M. V., Jones, C. & Liebmann, B. The South Atlantic convergence zone: Intensity, form, persistence, and relationships with intraseasonal to interannual activity and extreme rainfall. *J. Clim.* **17**, 88–108 (2004).
- Chug, D., Dominguez, F. & Yang, Z. The Amazon and La Plata River Basins as Moisture Sources of South America: Climatology and Intraseasonal Variability. *J. Geophys. Res.* **127**, e2021JD035455 (2022).
- Silva, G. A. M., Ambrizzi, T. & Marengo, J. A. Observational evidences on the modulation of the South American Low Level Jet east of the Andes according the ENSO variability. *Ann. Geophys.* **27**, 645–657 (2009).
- Hersbach, H. et al. The ERA5 global reanalysis. *Q. J. R. Meteorol. Soc.* **146**, 1999–2049 (2020).
- Wilks, D. S. *Statistical Methods in the Atmospheric Sciences*. vol. 91 (Second Edition, Academic Press, Inc. San Diego, California, USA, 2011).
- Jones, C. & Carvalho, L. M. V. Stochastic simulations of the Madden-Julian Oscillation activity. *Clim. Dyn.* **36**, 229–246 (2011).
- Jones, C. & Carvalho, L. M. V. Active and break phases in the South American Monsoon system. *J. Clim.* **15**, 905–914 (2002).
- Liebmann, B. Description of a Complete (Interpolated) Outgoing Longwave Radiation Dataset. *Bull. Am. Meteorol. Soc.* **77**, 1275–1277 (1996).
- Kiladis, G. N. et al. A comparison of OLR and circulation-based indices for tracking the MJO. *Mon. Weather Rev.* **142**, 1697–1715 (2014).
- Huffman, G. J., Stocker, E. F., Bolvin, D. T., Nelkin, E. J. & Tan, J. *GPM IMERG Final Precipitation L3 1 day 0.1 degree x 0.1 degree V06*. (2019).
- Funk, C. et al. The climate hazards infrared precipitation with stations—a new environmental record for monitoring extremes. *Sci. Data* **2**, 150066 (2015).

ACKNOWLEDGEMENTS

The ERA5 reanalysis were downloaded from the Research Data Archive at the National Center for Atmospheric Research, Computational and Information Systems Laboratory, Boulder, CO. [Available online at <https://rda.ucar.edu/datasets/ds620.0>]. The authors also thank the European Centre for Medium-Range Weather Forecasts

(ECMWF) for making the ERA5 reanalysis available for this research. The authors would like to thank the financial support from NSF (AGS 1937899).

AUTHOR CONTRIBUTIONS

C.J. defined the objectives of this study and was responsible for downloading the data and performing the analyses. He also wrote the initial versions of the paper. Y.M. processed IMERG and CHIRPS data and contributed to the analyses. L.M.V. Carvalho and Q.D. helped with literature review, results interpretation and manuscript revisions.

COMPETING INTERESTS

The authors declare no competing interests.

ADDITIONAL INFORMATION

Supplementary information The online version contains supplementary material available at <https://doi.org/10.1038/s41612-023-00501-4>.

Correspondence and requests for materials should be addressed to Charles Jones.

Reprints and permission information is available at <http://www.nature.com/reprints>

Publisher's note Springer Nature remains neutral with regard to jurisdictional claims in published maps and institutional affiliations.



Open Access This article is licensed under a Creative Commons Attribution 4.0 International License, which permits use, sharing, adaptation, distribution and reproduction in any medium or format, as long as you give appropriate credit to the original author(s) and the source, provide a link to the Creative Commons license, and indicate if changes were made. The images or other third party material in this article are included in the article's Creative Commons license, unless indicated otherwise in a credit line to the material. If material is not included in the article's Creative Commons license and your intended use is not permitted by statutory regulation or exceeds the permitted use, you will need to obtain permission directly from the copyright holder. To view a copy of this license, visit <http://creativecommons.org/licenses/by/4.0/>.

© The Author(s) 2023